RSC Advances

ROYAL SOCIETY OF CHEMISTRY

www.rsc.org/advances

RSC Advances

PAPER

Synthesis of α-aminophosphonates using a mesoporous silica catalyst produced from sugarcane bagasse ash

Received 00th January 20xx,
Accepted 00th January 20xx

DOI: 10.1039/x0xx00000x

www.rsc.org/

Arthur F. Boza[a], Vicente L. Kupfer[a], Aline R. Oliveira[b], Eduardo Radovanovic[a], Andrelson W. Rinaldi[a], Joziane G. Meneguin[a], Nelson L. C. Domingues[b], Murilo P. Moisés[ad], Sílvia L. Favaro[ac]*

A new approach to the green synthesis route has been proposed for obtaining a mesoporous material using sugarcane bagasse ash (SBCA) as silica source. The material obtained was denoted as SBA-16 and its mesostructure was characterized by low-angle X-ray diffraction (XRD), Fourier transform infrared spectroscopy (FTIR), scanning electron microscopy (SEM), transmission electron microscopy (TEM) and nitrogen adsorption techniques. Sulfonic acids groups was introduced in the as-synthesized material obtaining an acid catalyst denoted SBA-16/SO_3H. The catalytic activity of SBA-16 and SBA-16/SO_3H was investigated in Kabachnik-Fields reactions, where α-aminophosphonates compounds were produced. The results over the reactions shown that both products can be considered promising catalysts, where the SBA-16/SO_3H yielded a slight better performance than the SBA-16.

1 Introduction

Brazil has the largest area of sugarcane plantation in the world and is a leading exporter of their main products - sugar and ethanol. According to the available data, in 2014 Brazil has processed over 630 million tons of raw material producing about 35.5 million tons of sugar and 28.3 billion liters of ethanol.[1]

Sugarcane bagasse ash (SCBA) is generated as a byproduct of power plants from biomass burned. For each ton of sugarcane bagasse burned is generated about 6.2 kg of SCBA[2], which is composed mainly of silica.[3a] Some researchers reported the use of this byproduct in Portland cement,[3a,b] ceramic material[4] and zeolite synthesis.[5] Another use for this cheap silica source was reported in this work, it is the synthesis of SBA-16 type mesoporous silica.

Considering the porous materials, the SBA-16 type mesoporous silica (member of the Santa Barbara Amorphous family) has been reported with cubic arrangement corresponding to *Im3m* space group.[6] The synthesis of this material is usually performed under acid conditions using a non-ionic surfactant, Pluronic F127, as structure-directing agent and tetraethylorthosilicate (TEOS) as silica source.[6,7a-h,8,9]

The cage structure of SBA-16 has potential advantages for wide applications in different fields including catalysis,[7a-c] adsorption,[7d,e] electronics devices,[7f,g] and drugs delivery[7h] and the successfully modification of mesoporous silica surface by organic functionalities has been reported.[10a-e] In this context, sulfonic acid groups has been reported as an efficient acid catalyst in organic reactions i.e. α-aminophosphonates synthesis.[10e] The α-aminophosphonates belong to a class of compounds which have biological activities, which has drawn attention from researchers because of the vast area of application, such as pesticides, enzyme inhibitors, antiviral agents, antibiotics, drugs for the treatment of cancer and HIV proteases. Their synthesis has received considerable importance due to its structure similar to amino acids.[11]

Furthermore, the functionalization of environmentally friendly SBA-16 with sulfonic acids groups and the synthesis of α-aminophosphonates were investigated.

2 Experimental Section

1.1 Synthesis of SBA-16

Firstly, the sugarcane bagasse ash (SCBA) was collected from the sugar-alcohol plant located in the region of Maringá City, Paraná, Brazil. The alkali process was carried out for better extracting silicon from quartz structure. The SCBA was placed in a horizontal furnace and heated at a rate of 20 °C•min^{-1} from room temperature up to 600°C, and holding for 4 h (SCBA600). Furthermore the composition (weight percent) of SCBA found by XRF was 86.2% SiO_2, 2.8% Al_2O_3, 1.6% P_2O_5, 2.4% K_2O, 1.9% TiO_2, 1.5% CaO, 2.9% Fe_2O_3 and 0.7% of trace elements, and of SCBA600 was 92.0% SiO_2, 1.6% Al_2O_3, 1.1%

[a] Laboratory of Materials Chemistry and Sensors - LMSen, State University of Maringá - UEM, 5790 Colombo avenue, 87020-900, Maringá, PR, Brazil
[b] Laboratory of Catalysis and Biocatalysis Organic - LACOB, Federal University of the Grande Dourados - UFGD, Km 12 Dourados Itahum road, 79.804-970, Dourados - MS, Brazil.
[c] Department of Mechanical Engineering, State University of Maringá - UEM, 5790 Colombo avenue, 87020-900. Maringá, PR, Brazil. E-mail: slrosa@uem.br; Tel: +55-44-30111393.
[d] Federal Technological University of Paraná - UFTPR, 635 Marcílio street, 86812-460. Apucarana, PR, Brazil
DOI: 10.1039/x0xx00000x

P_2O_5, 1.0% K_2O, 0.6% TiO_2, 0.8% CaO, 1.5% Fe_2O_3, and 1.4% of trace elements were previously related.[5] The SCBA600 was used as the silica precursor to synthesis of SBA-16 where 4.0 g of SCBA600 were mixed with 6.0 g of NaOH (ratio of 1.5 w/w) to obtain a homogeneous mixture. Then, the mixture was heated in a nickel crucible at atmospheric pressure at 550°C for 40 minutes. The resultant fused mixture was dissolved in 50 mL of deionized water (solution 1). Then, 4.0 g of surfactant Pluronic F127 ($EO_{106}PO_{70}EO_{106}$, EO = ethylene oxide, PO = propylene oxide; Sigma Aldrich) was dissolved in 120 mL of HCl solution,
2 mol•L^{-1}, at room temperature. The mixture was stirred at room temperature until a homogeneous gel solution was formed (solution 2). Afterward, solution 2 was added to solution 1, and was kept under moderate stirring at room temperature for 20 h. The solid product was filtered, washed with deionized water, and air-dried at 80°C for 4 h. Finally, the as-prepared white powder was calcinated in air at 550°C for 6 h, with a heating ramp to reach 550°C of 1°C•min^{-1}, to remove the surfactant. The sample obtained was denoted by SBA-16.

1.2 Synthesis of functionalized SBA-16 sulfonic groups

The anchor of organic group into mesostructured silica surface occurred via post-synthesis procedure.[10a] Initially the SBA-16 was functionalized with thiol (RSH) group. It was carried out under batch reaction conditions using a 150 mL flask fitted with a stirrer, a thermometer and a reflux condenser at 60°C. In a typical reaction, 1.0 g SBA-16 was dissolved in 30 mL of toluene, then 1.0 mL of 3-mercaptopropyltrimethoxysilane (MPTMS) was added. After stirring for 24 h, the SBA-16 powder functionalized with thiol group was recovered as described in 2.1 item. Then, the thiol functionalized SBA-16 was oxidized with slowly dropwise of 30 mL of 30 wt% H_2O_2 solution for 24 h with moderate stirring at room temperature. The solid products were recovered, as described in 2.1 item and was denoted by SBA-16/SO_3H.

1.3 α-aminophosphonates synthesis

Initially the reactions were carried out varying the amount of catalysts (0.003, 0.006, 0.008, 0.01 and 0.02 g). In a typical reaction, 2.0 mmol of aniline, 2.2 mmol of benzaldehyde and 2.0 mmol of diphenylphosphite were mixed in blank reaction and with the presence of SBA-16 and SBA-16/SO_3H in amounts above indicated.
In next, the aminophosphonates was synthesized in similar way, where 0.01 g of catalysts was used in presence of different solvents (toluene, dichloromethane, chloroform, TFH, ethanol and methanol). Finally, establishing the standardization of reaction Kabachnik-Fields, other α-aminophosphonates were synthesized following the same protocol, but with benzaldehyde and aniline replaced as described in Figure 1.

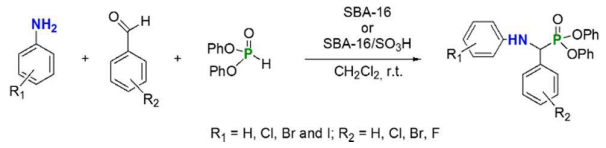

Figure 1 SBA-16 and SBA-16/SO_3H catalyzed in a general scope of the Kabachnik–Fields reactions.

1.4 Characterization Techniques

Low-angle X-ray diffraction XRD patterns were obtained using a Bruker D8-Advance equipment with Cu-Kα radiation, wavelength of 1.5406 Å, operated at 40 kV and 35 mA, 0.01° step size and 2 s/step time over range 0.5°< 2θ < 5°.
Nitrogen adsorption–desorption isotherms were measured at -196°C on a Quantachrome NOVA-1200E Surface and PoroAnalizer equipment. The specific surface areas were evaluated using Brunauer–Emmett–Teller (BET) method and the pore size distribution was calculated using the Barrett–Joyner–Halenda (BJH). Fourier transform infrared (FTIR) spectra were recorded with Thermo Fischer Scientific Nicolet IZ10 equipment in the range of 400-4000 cm^{-1} using KBr disc method. Scanning Electron Microscopy (SEM) images were obtained with Shimadzu SSX-550 Superscan equipment and Transmission Electron Microscopy (TEM) images were recorded on JEOL JEM-1400 equipment operated at 120 kV.
Acid capacities of SBA-16 and SBA-16/SO_3H were indicated by temperature-programmed ammonium desorption (NH3-TPD) and was carried out with AutoChem II 2920 equipment. The α-aminophosphonates products were characterized using ^1H and ^{13}C nuclear magnetic resonance spectroscopy (NMR), using $CDCl_3$ as solvent and, recorded on a 300 MHz Bruker AVANCE III HD spectrometer. Chemical shifts were expressed in parts per million (ppm) and coupling constants (J) were reported in Hertz (Hz).

2 Results and discussion

2.1 Structure characterization and Morphology

Figure 2(a) shows the powder X-ray diffraction patterns of SBA-16 and SBA-16/SO_3H prepared as described previously.

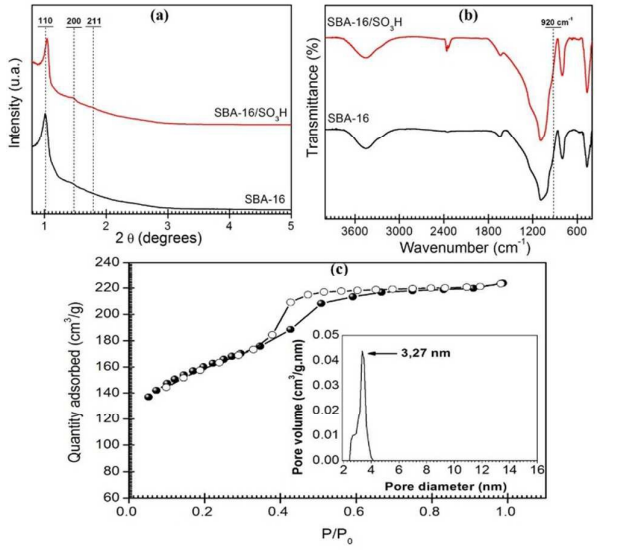

Figure 2 Powder XRD patterns (a) FTIR spectrum (b) of calcined SBA-16 and SBA-16/SO_3H and Nitrogen adsorption/desorption isotherms and pore size distribution of SBA-16 sample (c).

Table 1 Textural and structural properties of SBA-16

Sample	d_{110} (nm)	a_0 (nm)	S_{BET} ($m^2 \bullet g^{-1}$)	W (nm)	V_t (cm^3/g)	V_m (cm^3/g)	V_m/V_t (%)	D_p (nm)	Ref.
SBA-16	8.48	11.99	576	6.78	0.34	0.10	29	3.27	this work
SBA-16 STD	9.99	14.13	443	9.14	0.24	0.16	67	3.1	8

d_{110}: The plan spacing at Miller indices; a_0: the cubic lattice parameter ($a_0 = \sqrt{2} * d_{110}$); S_{BET}: BET surface area; W: wall thickness ($W = \sqrt{3}a_0/2 - D_p$); V_t: total pore volume; V_m: micropore volume calculated from BJH method; D_p: pore diameter.

Both shows a single intense diffraction peak at 2θ value of 1.01 and 1.04°, respectively, which belongs to cubic phase of (1 1 0) plan. The slight shift to higher 2θ in the peak position is due to the grafting of sulfonic acid groups into the SBA-16 pores.[12] From Bragg's law ($n\lambda = 2d \sin\theta$) and the relationships ($1/d_{hkl}^2 = (h^2 + k^2 + l^2)/a_0^2$) and ($a_0 = \sqrt{2}d_{110}$) between the cubic lattice parameter (a_0) and plane distance (d_{hkl}) at different Miller indices (hkl), if the first peak belongs to the (110) diffraction peak of cubic phase, the diffraction peaks should appear at $2\theta_{200}$=1.433° and $2\theta_{211}$=1.755°, for the SBA-16 and $2\theta_{200}$=1.47° and $2\theta_{211}$=1.80° for the SBA-16/SO_3H. Soon, our second diffraction peaks of experimental data match the theoretical results very well with 2θ = 1.425° and 1.471°, respectively, and to a third small peak for the SBA-16/SO_3H at 1.79°, only.

Therefore, XRD patterns of SBA-16 can be indexed as (1 1 0), (2 0 0), (2 1 1) reflections corresponding to a cubic Im3m structure.[7h] Figure 2(b) shows the Fourier transform infrared (FTIR) spectra of SBA-16 and SBA-16/SO_3H, which present the typical peaks related to groups of absorption of mesoporous silica network around of 3700-3100, 1300-1000, 1640, 960, 810, 460 cm^{-1}. The bands around 460 cm^{-1} and 810 cm^{-1} are assigned to the symmetric stretching and rocking modes of the Si–O–Si vibrations.

The broad band at 1300–1000 cm^{-1} (with peak around 1080 cm^{-1}) is assigned to the asymmetric stretching mode of the Si–O–Si moiety.[13a,b] The shoulder at 960 cm^{-1} is assigned to silanol groups existing in the structure of the material.

The broad band in 3100-3700 cm^{-1} is associated to -OH stretching vibration mode of silanol groups to the water's hydroxyl groups and the another band observed at 1640 cm^{-1} is assigned to the vibrations of adsorbed water molecules.[13c] The characteristic IR signals of the sulfonic acid group in the SBA-16/SO_3H sample are overlapped at 920 cm^{-1} (νS-O), 1425 cm^{-1} (ν_{as}S=O), in 3000-3222 cm^{-1} ($\nu_{(O-H)}$) and a clear assign at 2340–2360 cm^{-1} described as the first overtone of the O–H bending vibration mode of SO_3H groups engaged in a strong hydrogen bond.[13d]

The adsorption/desorption isotherms for SBA-16 is shown in Figure 2(c). The sample exhibit isotherms type IV with hysteresis adsorption/desorption type H2, according to the IUPAC classification, characteristic of mesoporous materials.[14] The textural and structural properties is shown in Table 1, wherein the pore wall thickness of SBA-16 is calculated by $W = \sqrt{3}a_0/2 - D_p$,[9] where a_0 and D_p are the cubic lattice parameter and the pore diameter, respectively.

The specific surface area of 576.11 $m^2 \bullet g^{-1}$ has a good approximation to the value obtained by conventional synthesis of SBA-16, i.e. those that use conventional silica source (338-526 $m^2 \bullet g^{-1}$).[8,9]

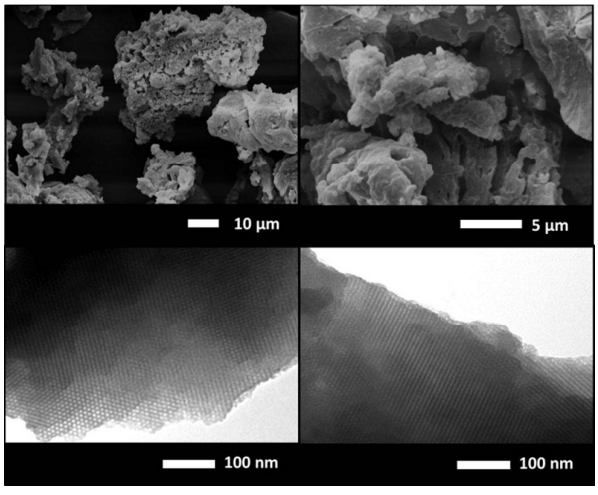

Figure 3 SEM image (up) and TEM images (down) of SBA-16 showing the characteristic plane for a cubic pore structure: (left) [111], right [100] direction.

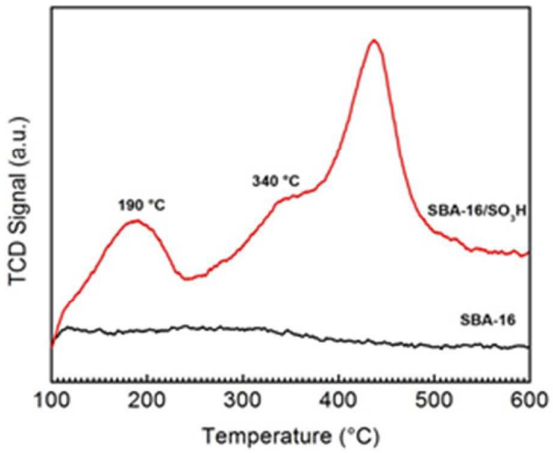

Figure 4 NH3-TPD curve of SBA-16 and SBA-16/SO_3H.

Table 2 Performance of different catalysts amounts in the α-aminophosphonates reactions[a]

Entry	Catalyst (g)	Time (min)	Yield (%)[b] SBA-16	Yield (%)[b] SBA-16/SO_3H
1	0.003	20	74	89
2	0.006	20	85	95
3	0.008	20	87	95
4	0.01	20	90	100
5	0.02	20	91	100

[a] Reaction conditions: aniline (2.0 mmol), benzaldehyde (2.2 mmol), diphenyl phosphite (2.0 mmol) in 10 mL solvent, room temperature.

[b] Isolated yields.

Moreover, the values of pore diameter (3.27 nm) and the percentage of micropore volume (29%) reaffirm the mesostructure of SBA-16.

SEM and TEM were employed for investigation of morphologic structure of SBA-16 (Figure 3). The up SEM images show the irregular morphology for SBA-16, synthetized without hydrothermal treatment. TEM images shows the pore structure along [1 1 1] direction (down-left image) and along [1 0 0] direction (down-right). Well-ordered cubic pore structure of 3–5 nm in diameter can be observed, corresponding to a cubic *Im3m* structure,[8] being this value in a good agreement with the analysis of XRD (Figure 2(a)) and N_2 physisorption (Figure(2c)).

On the other hand, a further increase in the catalyst loading up to 0.02 g did not confer any significant change on the yields.

Table 3 shows the influence of the solvents in the α-aminophosphonates synthesis. Both toluene, dichloromethane and chloroform presented the highest yields (Table 3, entries 1-3). So, we established the DCM as the standard solvent for further Kabachnik-Fields reactions using as starting materials diphenylphosphite (2.0 mmol), aniline 4-derivatives (2.0 mmol) and benzaldehyde 4-derivatives (2.2 mmol) in DCM using 0.01 g of the catalyst.

Figure 4 shows the NH_3-TPD curve of SBA-16 and SBA-16/SO_3H. A large desorption peak centered around 190 °C was observed.

Note that no desorption peak appeared in the NH_3-TPD curve of the unmodified SBA-16, which confirms that the peak for SBA-16/SO_3H is assigned to the NH_3 desorption from sulfonic acid groups. In addition, another peak between 250 to 500 °C occurs, but this indicates the decomposition of sulfonic acid groups in temperatures above 200 °C.[15]

1.2 Catalyst test

The blank reaction was carried out without the presence of catalyst per 60 minutes and has not obtained the compound of interest. Table 2 shows the performance of the α-aminophosphonates synthesis with the variations of the catalyst loading. The amount of SBA-16 and SBA-16/SO_3H varied from 0.003 to 0.02 g. The yields increased gradually until the catalyst's best performance of 0.01 g. Data of the remaining reactions are presented in Table 4 in a comparison of SBA-16 to SBA-16/SO_3H as heterogeneous catalysts (Tables 3 and 4). We could observe that the catalyst produced the α-aminophosphonates in good and excellent yields. So, concerning to the structural analysis of SBAs, the presence of the sulfonic group did not confer any considering improvement on the yields for Kabachnick-Fields reaction. Through the analysis of these data, we concluded that the catalysis was preferentially performed in the Brønsted acid sites. The presence of silanol group in the SBA-16 causes a density of positive charge attributed to the hydroxyl group that can beconsidered as a very weak Brønsted acid site[16].

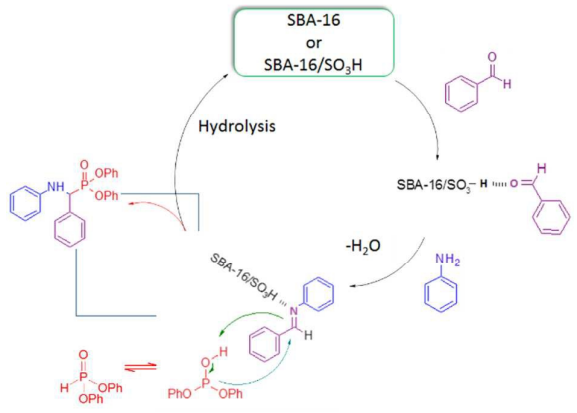

Figure 5 Plausible mechanism for the synthesis of α-aminophosphonates over a SBA-16 and SBA-16/SO_3H catalyst.

Table 3 Performance of solvents in the α-aminophosphonates reactions[a]

Entry	Solvents	Yield (%)[b]
1	Toluene	95
2	Dichloromethane	100
3	Chloroform	98
4	THF	87
5	Ethanol	70
6	Methanol	79

[a] Reaction conditions:aniline (2.0 mmol), benzaldehyde (2.2 mmol), diphenylphosphite (2.0 mmol), SBA-16 (0.01g), solvent (10 mL), room temperature, 20 minutes.

[b] Isolated yields.

Table 4 Synthesis of different α-aminophosphonates in presence of SBA-16 and SBA-16/SO_3H

Entry	Aldehyde	Amine	Product	SBA-16 (Yield[a]/Time[b])	SBA-16/SO_3H (Yield[a]/Time[b])
1	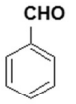	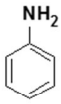	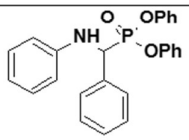	100 / 20	100 / 20
2	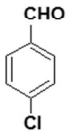	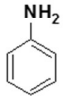	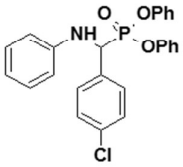	90 / 30	93 / 30
3	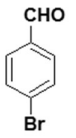	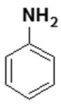	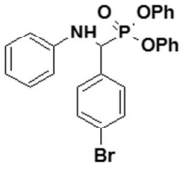	92 / 30	98 / 30
4	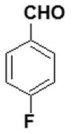	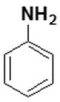	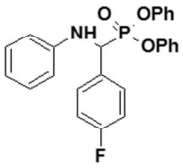	75 / 45	78 / 45
5	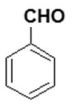	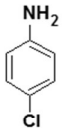	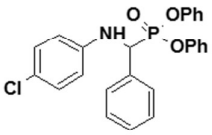	87 / 30	90 / 30
6	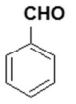	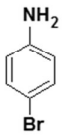	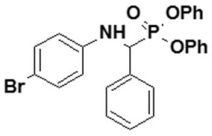	93 / 45	95 / 30

[a] Isolate yields (%)

[b] Time reaction (min)

On the other hand the SBA-16/SO_3H catalyst gives better performance in relation to SBA-16, which is expected because of its strong acid sites attributed to sulfonic acids groups, in accordance with TPD-NH_3 analysis. Besides, to the best of our knowledge, the imine synthesis (intermediate II) is the slow step for Kabachnick-Fields reactions.

So, we may infer that the presence of the catalyst resulted in an improvement on the reaction rate for synthesis step of this intermediate. With this information, we purposed a plausible mechanism for those reactions. Firstly, the benzaldehyde will interact with SBA, specifically in the Brønsted acid sites (intermediate I). Secondly, the aniline will attack the intermediate I and, after the water's removal, the imine's intermediate is obtained (intermediate II). After this step, the intermediate II will undergo an attack of the phosphite which will produce the α-aminophosphonate. The plausible mechanism was in accordance with the literature and it is showed in the Figure 5.[17a-b]

The products and results of the synthesis of α-aminophosphonates using heterogeneous catalysts SBA-16 and SBA-16/SO_3H are given in Table 4.

Conclusions

In the present work, we have proposed a new approach to the synthesis of SBA-16 type mesoporous silica from the sugarcane bagasse ash. The as-synthesized material has good textural and structural properties, being a good alternative to the use of SCBA. Furthermore, the material obtained was successfully functionalized with sulfonic acid groups allowing the improvement of its catalytic activity for the α-aminophosphonates synthesis.

Acknowledgements

We gratefully acknowledge the Brazilian agencies (CAPES/CNPQ) for financial support.

Notes and references

1 ÚNICA, *União da Indústria da Cana de Açúcar,* 2015, http://www.unicadata.com.br
2 FIESP/CIESP report 2001, http://www.fiesp.com.br/arquivo-download/?id=4505
3 (a) G. C. Cordeiro, R. D. Toledo Filho, E. M. R. Fairbairn, *Construction and Building Materials,* 2009, **23**, 3301–3303; (b) M. Frías, E. Villar, H. Savastano, *Cement & Concrete Composites*, 2011, **33**, 490-496.
4 A. E. Souza, S. R. Teixeira, G. T. Santos, F. B. Costa, E. Longo, J. Environ. Manage., 2011, **92(10)**, 2774-2780.
5 M. P. Moisés, C. T. P. Silva, J. G. Meneguin, E. M. Girotto, E. Radovanovic, *MaterialsLetters*, 2013, **108**, 243-246.
6 D. Zhao, Q. Huo, J. Feng, B. F. Chmelka, G. D. Stucky, *J. Am. Chem. Soc.*, 1998, **120**, 6024-6036.
7 (a) R. Huirache-Acuña, B. Pawlec, E. Rivera-Muñoz, R. Nava, J. Espino, J. L. G. Fierro, *Applied Catalysis B: Environmental*, 2009, **92**, 168-184; (b) S. Kataoka, A. Endo, A. Harada, Y. Inagi, T. Ohmori, *Applied Catalysis A: General*, 2008, **342**, 107-112; (c) R. Nava, B. Pawelec, P. Castaño, M. C. Álvarez-Galván, C. V. Loricera, J. L. G. Fierro, *Applied Catalysis B: Environmental*, 2009, **92**, 154-167; (d) W. J. Son, J. S. Choi, W. S. Ahn, *Microporous and Mesoporous Materials,* 2008, **113**, 31-40; (e) S. M. L. Santos, K. A. B. Nogueira, M. S. Gama, J. D. F. Lima, I. J. Silva, D. C. S. Azevedo, *Microporous and Mesoporous Materials*, 2013, **180**, 284-292; (f) T. Yamada, H. S. Zhou, H. Uchida, I. Honma, T. Katsube, *Phys. Chem. B*, 2004, **108(35)**, 13341–13346; (g) J. Tu, R. Wang, W. Geng, X. Lai, T. Zhang, N. Li, N. Yue, X. Li, *Sensors and Actuators B: Chemical*, 2009, **136**, 392-398; (h) Y. Hu, J. Wang, Z Zhi, T. Jiang, S. Wang, *J Colloid Interface Sci.*, 2011, **363**, 410-417.
8 C. F. Cheng, Y. C. Lin, H. H. Cheng, Y. C. Chen, *Chemical Physics Letters*, 2003, **382**, 496-501.
9 M. A. Ballem, J. M. Córdoba, M. Odén, *Microporous and Mesoporous Materials*, 2010, **129**, 106-111.
10 (a) C. Pirez, A. F. Lee, J. C. Manayil, C. M. A. Parlett, K. Wilson, *Green Chemistry*, 2014, **16**, 4506-4509; (b) A. Mansoor andS. Salehi, *Dyes and Pigments*, 2012, **94**, 1-9; (c) A. Giuseppe, C. Nicola, R. Pettinari, I. Ferino, D. Meloni, M. Passacanto, M. Cruicianelli, *Catal. Sci. Technol.*, 2013, **3**, 1972-1984; (d) C. T. Tsai, Y. C. Pan, C. C. Ting, S. Vetrivel, A. S. T. Chiang, G. T. K. Fey, H. M. Kao, Chem. Commun., 2009, 5018–5020. (e) G. M. Ziarani, N. Lashgari, A. Badiei, *Journal of Molecular Catalysis A: Chemical*, 2015, **397**, 166-191.
11 Y. Zhang and C. Zhu, *Catalysis Communications*, 2012, **28**, 134-137.
12 B. Rác, A. Molnár, P. Forgo, M. Mohai, I. Bertóti, *Journal of Molecular Catalysis A: Chemical*, 2006, **244**, 47-57.
13 (a) J. Wang, B. Zou, M. A. El-Sayed, *Journal of Molecular Structure*, 1999, **508**, 87-96; (b) C. T. Kirk, *Physical Review B*, 1988, **38(2)**, 1255-1273; (c) S. N. Azizi, S. Ghasemi, H. Yazdani-Sheldarrei, *International Journal of Hydrogen Energy*, 2013, **38**, 12774–12785; (d) G. G. Kumar, P. Uthirakumar, K. S. Nahn, R. N. Elizabeth, *Solid State Ionics*, 2009, **180**, 282-287.
14 K. S. W. Sing, *Pure Appl. Chem*., 1982, **54(11)**, 2201-2218.
15 K. Shimizu, E. Hayashi, T. Hatamachi, T. Kodama, T. Higuchi, A. Satsuma, Y. Kitayama, *Journal of Catalysis*, 2005, **231**, 131-138.
16 M. J. Climent, A. Corma, S. Iborra, *RSC Advanves*, 2012, **2**, 16-58.
17 (a) S. A. R. Mulla, M. Y. Pathan, S. S. Chavan, S. P. Gample, D. Sarkar, *RSC Advances*, 2014, **4**, 7666-7672; (b) A. Srivani, P. S. Sai Prasad, N. Lingaiah, *Catal. Lett.*, 2012, **142**, 389-396.

Graphical Abstract